

# Supporting Information for ”Dynamics of a Solidifying Icy Satellite Shell”

J. J. Buffo<sup>1</sup>, C. R. Meyer<sup>1</sup>, and J. R. G. Parkinson<sup>2</sup>

<sup>1</sup>Thayer School of Engineering, Dartmouth College, Hanover, NH 03755, USA

<sup>2</sup>Atmospheric, Oceanic and Planetary Physics, Department of Physics, Clarendon Laboratory, University of Oxford, Parks Road,

Oxford OX1 3PU, UK

## Contents of this file

1. Text S1 to S4
2. Figures S1 to S4
3. Movies S1 to S2

## Introduction

Below we include four supplementary sections which aim to bolster the conclusions of the main manuscript. Section S1 provides an independent validation of the two-dimensional multiphase reactive transport model (SOFTBALL (Parkinson et al., 2020)) utilized throughout the work via simulations of sea ice growth. Section S2 supports the implementation of a linear conductive profile approximation for estimating the ice-ocean interface thermal gradient by comparing simulated and approximated ice shell thermal profiles. Section S3 builds on and supports the work of Section 3.3 of the main manuscript by comparing the brine channel spacing produced under European conditions to those predicted by contemporary models simulating terrestrial ice-ocean/brine environments (Wells

---

et al., 2011; Parkinson, 2019). Section S4 discusses potential limitations of the single domain Darcy velocity approach for investigating the geometry and longevity of brinicles.

### **Text S1 - Model Validation**

To independently validate the two-dimensional reactive transport model of Parkinson et al. (2020) we simulated the physicochemical evolution of sea ice under simplified polar conditions. Model runs were initiated by assuming the domain was entirely filled with seawater (35 ppt) just above its melting temperature ( $-1.68\text{C}$ ), subject to an undercooled atmosphere above ( $-23.15\text{C}$ ) and an ambient ocean below ( $-1.68\text{C}$ ). To ensure the model produces consistent results across a range of spatial scales (important for our upscaling to the Europa environment), we carried out four different runs at varying resolutions, the results of which can be seen in Figure S1. While it is clear that the detailed structure of brine channels within the ice layer are less well resolved when a coarser resolution is employed, the overall bulk salinity profile of the ice is maintained across all resolutions. This can be seen by horizontally averaging the two-dimensional bulk concentration profiles of Figure S1. The results of such an averaging can be seen in Figure S2, which depicts bulk salinity profiles for all four simulated resolutions of Figure S1. There exists only minor variations in bulk salinity, primarily near the ice-ocean interface, where the coarsest resolution simulation struggles to resolve details of the phase change interface between 0.75-0.85 m. Additionally, the simulated bulk salinity profiles qualitatively and quantitatively match empirical measurements of both natural and laboratory grown sea ice (e.g. (Eicken, 1992; Nakawo & Sinha, 1981; Notz et al., 2005)), exhibiting a characteristic ‘c-shape’ salinity profile with amplified salinities near both the upper ice-atmosphere interface and the basal ice-ocean interface as well as bulk salinity values well within the observational range (Eicken, 1992; Nakawo & Sinha, 1981; Notz et al., 2005). The ability of the model to reproduce bulk salinity profiles of sea ice provides an additional and

independent validation of the model, expanding upon the existing literature (Parkinson, 2019; Parkinson et al., 2020; Wells et al., 2019), and lending confidence to the model’s application to planetary ice-ocean systems.

### **Text S2 - Ice Shell Thermal Profile**

To demonstrate the validity of implementing the simple linear conduction approximation for the ice-ocean interface thermal gradient (Equation 7 of the main text), we compare the thermal profile during a selected simulation to that predicted by the linear conduction approximation:

$$T(z) = T_s + \frac{T_{oc} - T_s}{H_{shell}}z \quad (1)$$

where  $z$  is depth beneath the surface,  $T_{oc}$  is ocean temperature,  $T_s$  is the surface temperature, and  $H_{shell}$  is the thickness of the ice shell. The results of this comparison can be seen in Figure S3. The profiles vary only slightly, with true temperatures being slightly higher throughout the majority of the shell. This is an expected result as the ice-ocean interface mushy layer will buffer heat loss to the cold upper surface due to the lower thermal conductivity of brine compared to ice. Such variations in ice shell thermal profiles have previously been shown to have a negligible affect on interface dynamics and ice shell physicochemical characteristics (Buffo et al., 2020).

### **Text S3 - Brine Channel Spacing**

The distribution of brine channels in the mushy layer plays a fundamental role in the desalination and structure of the ice-ocean interface, and thus the physicochemical properties of ocean-derived ices. Channel spacing is a dynamic property and depends on a number of environmental pressures which control convective motion in the porous region near the ice-ocean phase boundary. Brine channel spacing in saltwater systems has previously been investigated, both experimentally (Wakatsuchi & Saito, 1985; Tison &

Verbeke, 2001) and theoretically (Wells et al., 2011; Parkinson, 2019). Wells et al. (2011) and Parkinson (2019) demonstrate that the non-dimensional brine channel aspect ratio, defined as:

$$a_s = \frac{L}{2h} \quad (2)$$

where  $L$  is the horizontal distance between brine channels and  $h$  is the thickness of the ice-ocean interface mushy layer, is strongly controlled by the mush Rayleigh number (Wells et al., 2011; Parkinson, 2019):

$$Ra_{ML} = \frac{K_0 \rho_{br} g \beta \Delta C h}{\kappa_{br} \eta} \quad (3)$$

where  $K_0$  is a characteristic permeability,  $\rho_{br}$  is the density of the underlying ocean/brine,  $g$  is gravity,  $\beta$  is the solutal contraction coefficient,  $\Delta C$  is the difference in salinity between the eutectic concentration and the underlying fluid,  $h$  is mushy layer thickness,  $\kappa_{br}$  is the thermal diffusivity of the underlying fluid, and  $\eta$  is dynamic fluid viscosity.

To investigate the relationship between ice-ocean interface environment and brine channel spacing, in both planetary and terrestrial systems, we measured brine channel aspect ratios for seven simulations (ice shell depths ranging from 10 m to 1000 m) under European conditions and compare our results to those of Wells et al. (2011) and Parkinson (2019) (Figure S4). Additionally, we measured brine channel aspect ratios during a simulation of sea ice to ensure our results agree with those of Parkinson (2019) who simulate the top-down solidification of sea ice under a range of thermal forcing and during a simulation where a concentration ratio  $\mathcal{C}=1$  is implemented to bridge the existing gap between the concentration ratios investigated by Wells et al. (2011) ( $\mathcal{C}=2,5,10,15$ ) and those utilized

in Parkinson (2019) and the current work ( $\mathcal{C}=0.18$ ). Following Wells et al. (2011), the concentration ratio is defined as:

$$\mathcal{C} = \frac{C_0 - C_s}{C_e - C_0} \quad (4)$$

where  $C_0$  is the salinity of the underlying fluid,  $C_s$  is the salinity of ice (here taken to be zero), and  $C_e$  is the eutectic concentration.

Our simulation results, as well as the results of Wells et al. (2011) and Parkinson (2019), show a general trend of decreasing brine channel aspect ratio with increasing mush Rayleigh number, approaching a steady state value for  $Ra_{ML} \gg Ra_c$ , as reported by Wells et al. (2011), where  $Ra_c$  is the critical Rayleigh number where mushy layer convection initiates. This suggests that after onset of convection in the mushy layer the rate of mushy layer thickening (increasing  $h$ ) outpaces the collapse/merging of brine channels (a phenomenon well documented in the literature by both experimental and modeling studies, which leads to increasing  $L$ ), until a steady state aspect ratio is achieved. The primary environmental factor affecting the value of the steady state aspect ratio is the concentration ratio, for while simulations of sea ice and European ice had substantially different environmental forcing (gravity, characteristic permeability) their steady state aspect ratios vary minimally when compared to the difference in steady state aspect ratios of simulations with variable concentration ratios. An additional control on brine channel spacing is the finite width of our simulation domain, which necessarily quantizes the number of brine channels. We have taken care to select domain widths which facilitate a large number of brine channels whenever possible to reduce the impact of this numerical limitation. Another interesting feature of the simulations presented in Figure S4 is the existence of convective modes; apparent in all simulations except those of Wells et al. (2011), due to their method of selecting  $L$  such that it maximized solute flux from the

mushy layer (Wells et al., 2012) and observing the evolution of  $h$ , as jumps between well defined groupings that are well represented by the inverse fits of Figure S4 (additionally, transition between convective modes can be seen in Supplementary Movie S1 and S2 as brine channels collapse and reform). This alternation between quasi-stable convective modes in a confined porous media is a well documented natural phenomenon (e.g. (Karani & Huber, 2017)) which we believe is amplified by the finite resolution of the simulations. That is, as the resolution is coarsened, as is needed to simulate thicker mushy layers deep within the ice shell of Europa, the lower modes (associated with smaller aspect ratios) are likely not explicitly resolved by the simulation. This does not affect the accuracy of the physicochemical results of the model, however, as it was shown in Section S1 that bulk salinity profiles remain constant regardless of whether discrete brine channels are resolved (e.g. Figures S1 S2).

Due to the rapid rate at which ice-ocean systems exceed their critical Rayleigh numbers (e.g. the presence of brine channels in thin sea ice (Wettlaufer et al., 1997; Cox & Weeks, 1974)) we conclude that the thick ice shells of icy worlds such as Europa should have ice-ocean interfaces characterized by brine channel aspect ratios near their steady state limit. This suggests progressively widening channel spacing as the ice shell thickens that will scale with mushy layer thickness. Given the results of Section 3.2 of the main manuscript (that mushy layer thickness can be well approximated as a linear function of ice shell thickness, linear relationship coefficient=0.0539), and noting that the steady state brine channel aspect ratio is 0.08 (Blue lines of Figure S4), European ice shells of thickness 1 km, 10 km, and 30 km would have expected brine channel spacing of 8.62 m, 86.2 m, and 259 m, respectively. Constraining channel spacing is important in understanding the desalination and heterogeneity of the lower ice shell, which may have

substantial implications for the geophysical processes and habitability of ice-ocean worlds, as outlined in the main manuscript.

#### **Text S4 - A Note on Simulated Brinicle Geometry**

It is important to note that the geometry of the brinicles simulated in Section 3.3 may be impacted by the Darcy approximation implemented in the SOFTBALL code. The Darcy technique is employed to simplify the ice-ocean system and involves simulating the entire domain (liquid and solid) as a porous media (rather than solving Darcy's law in the porous region and the Navier-Stokes equation in the fluid). This is a widely used method and its accuracy hinges on the large amplification of permeability in the fluid region (compared to the porous region). A large, but finite, permeability means flow is faster in the fluid than in the porous region (ensuring accurate evolution of the multiphase layer), while still being computationally tractable and avoiding a difficult boundary value problem. The reduction of flow speed in the free fluid from its true value (permeability  $\neq$  infinity), however, means that diffusive processes are likely overly expressed in the fluid region. This could lead to amplified spacing between brinicle walls beneath downwelling high salinity regions (e.g. Figure 6). In the real system downwelling plumes will not be subject to a finite permeability and are likely to be more jet-like, reducing dissipative flow near the interface and potentially supporting more stable, longer-lived ice structures than suggested in Section 3.3 (See Wells et al. (2019)). We therefore suggest our results be taken as a lower limit for the longevity of brinicle structures at Europa's ice-ocean interface.

#### **Movie S1.**

Nondimensional bulk salinity evolution under European conditions. (Domain: 20m x 20m (512 x 512 grid), Resolution: 3.9cm)

#### **Movie S2.**

Porosity evolution under European conditions. (Domain: 20m x 20m (512 x 512 grid), Resolution: 3.9cm)

## References

- Buffo, J. J., Schmidt, B. E., Huber, C., & Walker, C. C. (2020). Entrainment and dynamics of ocean-derived impurities within europa's ice shell [Journal Article]. *JGR: Planets*.
- Cox, G. F. N., & Weeks, W. F. (1974). Salinity variations in sea ice [Journal Article]. *Journal of Glaciology*, 13(67), 109-120.
- Eicken, H. (1992). Salinity profiles of antarctic sea ice: field data and model results [Journal Article]. *Journal of Geophysical Research: Oceans*, 97(C10), 15545-15557.
- Karani, H., & Huber, C. (2017). Transitional behaviour of convective patterns in free convection in porous media [Journal Article]. *Journal of Fluid Mechanics*, 818.
- Nakawo, M., & Sinha, N. K. (1981). Growth rate and salinity profile of first-year sea ice in the high arctic [Journal Article]. *Journal of Glaciology*, 27(96), 315-330.
- Notz, D., Wettlaufer, J. S., & Worster, M. G. (2005). A non-destructive method for measuring the salinity and solid fraction of growing sea ice in situ [Journal Article]. *Journal of Glaciology*, 51(172), 159-166.
- Parkinson, J. R. G. (2019). *Nonlinear convection in sea ice and other mushy layers* (Thesis). University of Oxford.
- Parkinson, J. R. G., Martin, D. F., Wells, A. J., & Katz, R. F. (2020). Modelling binary alloy solidification with adaptive mesh refinement [Journal Article]. *Journal of Computational Physics: X*, 5, 100043.
- Tison, J.-L., & Verbeke, V. (2001). Chlorinity/salinity distribution patterns in experimental granular sea ice [Journal Article]. *Annals of Glaciology*, 33, 13-20.
- Wakatsuchi, M., & Saito, T. (1985). On brine drainage channels of young sea ice [Journal

- Article]. *Annals of glaciology*, 6, 200-202.
- Wells, A. J., Hitchen, J. R., & Parkinson, J. R. (2019). Mushy-layer growth and convection, with application to sea ice [Journal Article]. *Philosophical Transactions of the Royal Society A*, 377(2146), 20180165.
- Wells, A. J., Wettlaufer, J., & Orszag, S. (2011). Brine fluxes from growing sea ice [Journal Article]. *Geophysical Research Letters*, 38(4).
- Wells, A. J., Wettlaufer, J. S., & Orszag, S. A. (2012). Nonlinear mushy-layer convection with chimneys: stability and optimal solute fluxes [Journal Article]. *arXiv preprint arXiv:1205.0964*.
- Wettlaufer, J., Worster, M. G., & Huppert, H. E. (1997). Natural convection during solidification of an alloy from above with application to the evolution of sea ice [Journal Article]. *Journal of fluid mechanics*, 344, 291-316.

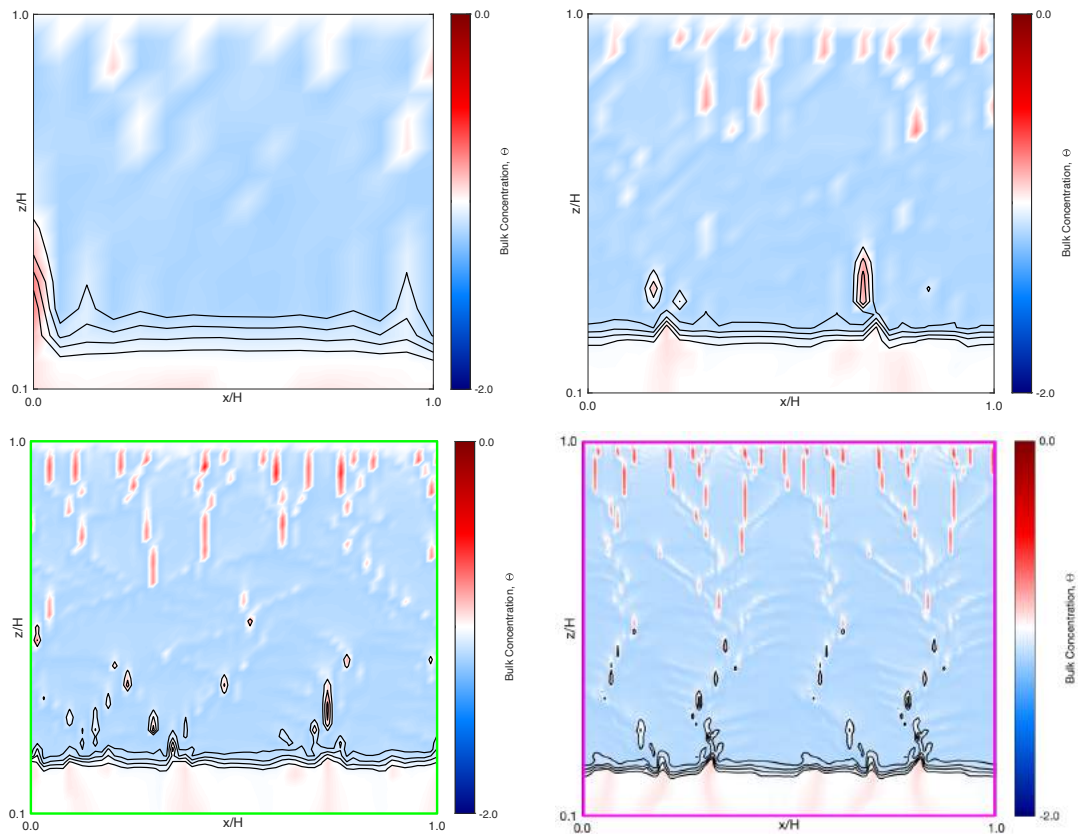


**Figure S1.** The effects of variable resolution. **Top Left)** 16x16 starting grid, no Adaptive Mesh Refinement (AMR) (6.25 cm resolution). **Top Right)** 32x32 starting grid, no AMR (3.13 cm resolution). **Bottom Left)** 32x32 starting grid, 1 level AMR (1.56 cm resolution). **Bottom Right)** 32x32 starting grid, 2 level AMR (0.78 cm resolution).

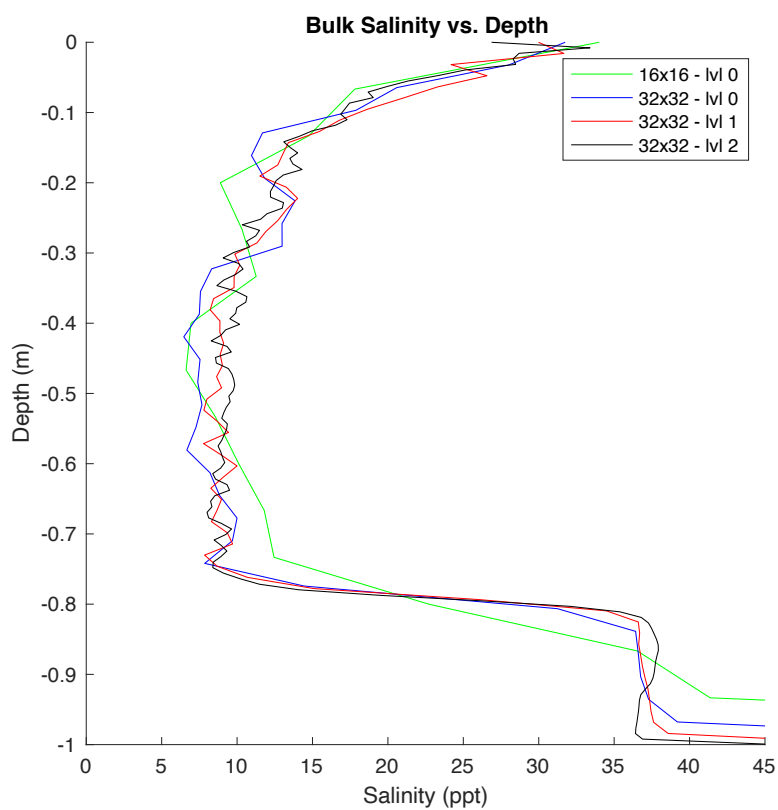


**Figure S2.** Horizontally averaged bulk salinity profiles. Using the results of Figure S1, bulk salinity is horizontally averaged and compared. Profiles have characteristic ‘c-shape’ of first year sea ice, with appropriate bulk salinity values, and are in good agreement across all resolutions.

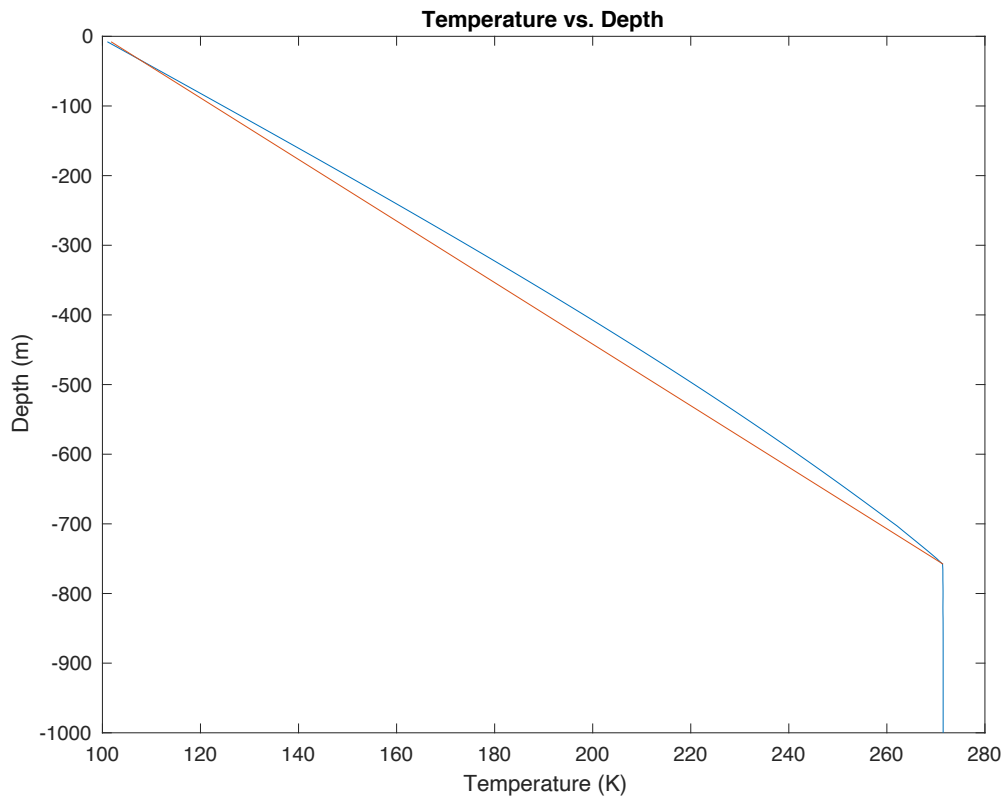


**Figure S3.** Thermal profiles in an ice shell. The blue curve is the horizontally averaged temperature profile extracted from a top-down solidification simulation under Europa conditions. The ice-ocean interface occurs at  $\sim 758$  m below the surface. The red curve is the linear conduction approximation given by Equation S1.

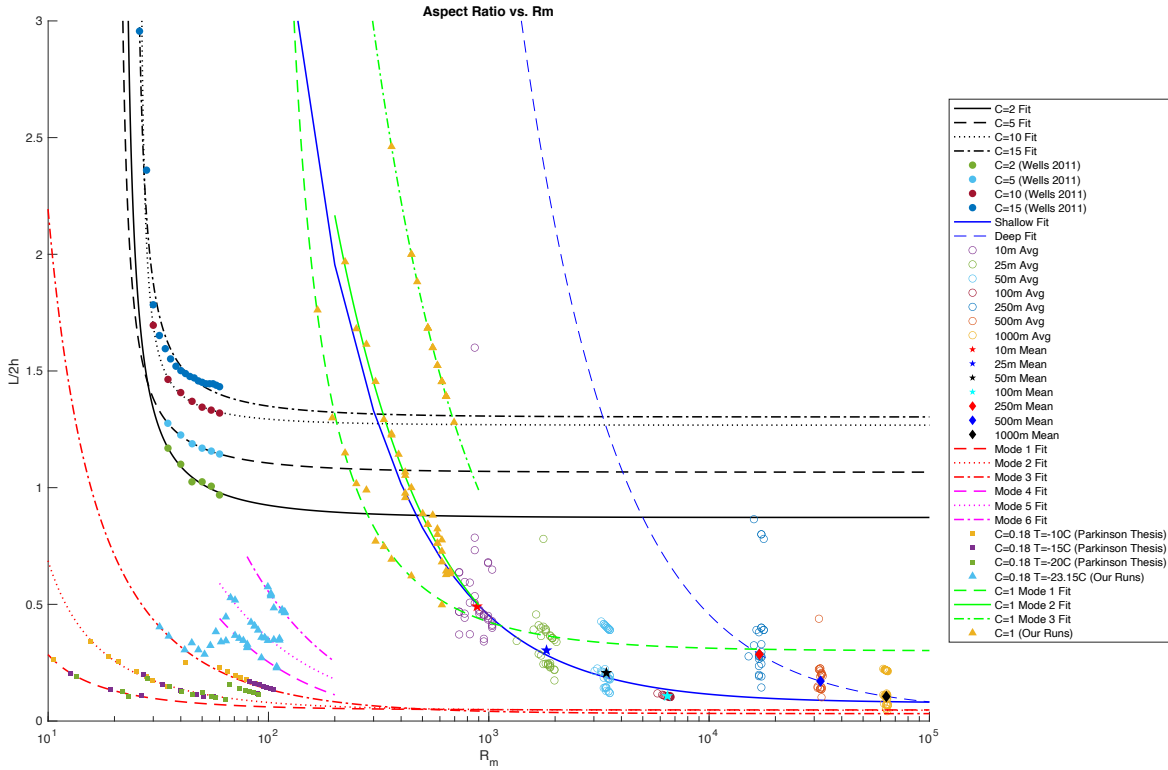


**Figure S4.** Brine channel aspect ratio as a function of mush Rayleigh number. Solid circles are results from Wells et al. (2011) and black curves are inverse fits to this data. Solid squares are results from Parkinson (2019) (Chapter 5.1.5) and red curves are inverse fits to this data. Open circles and solid stars/diamonds are simulation results and mean values for European environments runs, respectively, and blue curves are inverse fits to this data. Blue and yellow solid triangles correspond to our sea ice and  $\mathcal{C} = 1$  simulations, respectively, and the pink and green curves are their associated inverse fits. As the mush Rayleigh number increases brine channel aspect ratios approach a steady state value primarily governed by the concentration ratio, in agreement with the results of (Wells et al., 2011). ‘Modes’, as listed in the figure legend, are associated with mushy layer convective modes within simulation domains. These quasi-steady states are a common feature of convection in a confined porous media (Karani & Huber, 2017) and are amplified by the finite resolution of simulations.